Acta Pharmaceutica Sinica B 2022;12(7):3063–3072

Chinese Pharmaceutical Association
Institute of Materia Medica, Chinese Academy of Medical Sciences

Acta Pharmaceutica Sinica B

www.elsevier.com/locate/apsb
www.sciencedirect.com

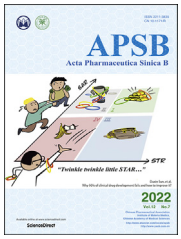

ORIGINAL ARTICLE

Activating Connexin43 gap junctions primes adipose tissue for therapeutic intervention

Yi Zhu[a,g,*], Na Li[a], Mingyang Huang[g], Xi Chen[g], Yu A. An[a], Jianping Li[b], Shangang Zhao[a], Jan-Bernd Funcke[a], Jianhong Cao[c], Zhenyan He[c], Qingzhang Zhu[a], Zhuzhen Zhang[a], Zhao V. Wang[b], Lin Xu[d,e], Kevin W. Williams[c], Chien Li[f], Kevin Grove[f], Philipp E. Scherer[a,h,*]

[a]*Touchstone Diabetes Center, Department of Internal Medicine, the University of Texas Southwestern Medical Center at Dallas, Dallas, TX 75390, USA*
[b]*Division of Cardiology, Department of Internal Medicine, the University of Texas Southwestern Medical Center at Dallas, Dallas, TX 75390, USA*
[c]*Division of Hypothalamic Research, Department of Internal Medicine, the University of Texas Southwestern Medical Center at Dallas, Dallas, TX 75390, USA*
[d]*Quantitative Biomedical Research Center, Department of Population and Data Sciences, the University of Texas Southwestern Medical Center at Dallas, Dallas, TX 75390, USA*
[e]*Department of Pediatrics, the University of Texas Southwestern Medical Center at Dallas, Dallas, TX 75390, USA*
[f]*Novo Nordisk Research Center, Seattle, WA 98109, USA*
[g]*Children's Nutrition Research Center, Department of Pediatrics, Baylor College of Medicine, Houston, TX 77030, USA*
[h]*Department of Cell Biology, the University of Texas Southwestern Medical Center at Dallas, Dallas, TX 75390, USA*

Received 30 October 2021; received in revised form 16 January 2022; accepted 8 February 2022

KEY WORDS

GJA1;
Adipose tissue;
Gap junction;
Connexin43;
FGF21;

Abstract Adipose tissue is a promising target for treating obesity and metabolic diseases. However, pharmacological agents usually fail to effectively engage adipocytes due to their extraordinarily large size and insufficient vascularization, especially in obese subjects. We have previously shown that during cold exposure, connexin43 (Cx43) gap junctions are induced and activated to connect neighboring adipocytes to share limited sympathetic neuronal input amongst multiple cells. We reason the same mechanism may be leveraged to improve the efficacy of various pharmacological agents that target adipose tissue. Using

*Corresponding authors. Tel.: +1 214 6488715.
E-mail addresses: Philipp.Scherer@UTSouthwestern.edu (Philipp E. Scherer), Yi.Zhu@bcm.edu (Yi Zhu).
Peer review under responsibility of Chinese Pharmaceutical Association and Institute of Materia Medica, Chinese Academy of Medical Sciences.

https://doi.org/10.1016/j.apsb.2022.02.020

β_3-Adrenergic receptor agonist;
Obesity;
Type 2 diabetes

an adipose tissue-specific Cx43 overexpression mouse model, we demonstrate effectiveness in connecting adipocytes to augment metabolic efficacy of the β_3-adrenergic receptor agonist Mirabegron and FGF21. Additionally, combing those molecules with the Cx43 gap junction channel activator danegaptide shows a similar enhanced efficacy. In light of these findings, we propose a model in which connecting adipocytes *via* Cx43 gap junction channels primes adipose tissue to pharmacological agents designed to engage it. Thus, Cx43 gap junction activators hold great potential for combination with additional agents targeting adipose tissue.

1. Introduction

According to the Centers for Disease Control and Prevention in 2019, more than 42% of U.S. adults fall into the obese category. Obesity is a major risk factor for many chronic diseases, including the most common comorbidity—type two diabetes (T2D)[1]. In the past three decades, many classes of pharmacological agents have been introduced to treat T2D[2]. However, most of them fall short of efficacy or have, at the concentrations used, undesirable side effects[3]. Therefore, there is still a need to improve the efficacy of existing agents or to develop new agents based on novel insights gained from mechanisms leading to obesity and T2D.

The problem underlying obesity and its sequelae is the imbalance of energy intake and expenditure. Conceptual strategies to restore this balance are straightforward: reduce energy intake, increase energy expenditure, or both. However, pharmacological interventions have encountered challenges on both fronts: strategies aimed to reduce food intake frequently affect hedonic reward mechanisms, leading to depression and even suicides; strategies aimed to increase energy expenditure, however, tend to lead to undesired cardiac toxicity or hyperthermia[4].

White adipose tissue regulates numerous physiological processes. It initially expands to store excess calories, but gradually becomes dysfunctional and contributes in a major way to the pathogenesis of metabolic diseases along with the progression of obesity[5]. Targeting adipose tissue is therefore a promising strategy to combat metabolic diseases[6]. Of the many mechanisms that adipose tissue can be engaged in to improve metabolic function, the induction and activation of thermogenic beige adipocytes within the white adipose depots has gained a lot of attention[7,8], in part for its benefits in dissipating excess energy, in part for its secretion of beneficial adipokines that enhance whole-body metabolism.

These recruitable beige adipocytes were first discovered by exposing mice to cold temperatures[8]. They were characterized as a new subtype of adipocyte in white adipose tissue depot in mice, resembling human supraclavicular brown adipocytes in gene expression[9], and capable of dissipating energy through their thermogenic program[8]. However, obesity or aging significantly impairs cold-induced recruitment of those thermogenic adipocytes in mice[10]. This echoes a similar clinical conundrum in humans[11,12]. Adipocytes become hypertrophied and insufficiently vascularized in obese patients[5], resulting in insufficient tissue blood perfusion[13] and difficulty for pharmacological agents to reach their target[6]. For example, mirabegron, an U.S. Food and Drug Administration (FDA)-approved β_3-adrenergic receptor (AR) agonist for overactive bladder, has not been approved to treat obesity and metabolic diseases, due to its lack of efficacy at the doses currently approved by the FDA. While increasing the doses can efficiently activate energy expenditure and recruit thermogenic adipocytes in the human subjects[14,15], it also leads to dose-dependent undesirable effects on blood pressure and heart rates[15]. Other β_3-AR agonists suffer from similar issues[16–19]. Similarly, FGF21 shows promising results in animal models by improving adipose tissue insulin sensitivity[20] and beiging[21], but unfortunately, these metabolic effects do not sufficiently translate in human studies with trials either showing limited[22] or no[23] efficacy on glycemic control. Here, we argue this lack of efficacy is partly due to insufficient targeting of adipose tissue by FGF21, even at maximal doses. Once we can overcome this obstacle, FGF21 may find a more clear-cut route to clinical use for the treatment of obesity and T2D.

Adipocyte gap junctions play an important role in adipose tissue physiology. Connexin43 (Cx43) is the most abundant connexin in adipocytes, and its activity is modulated by a number of different inputs. We have previously shown that adipose tissue Cx43 is increased by cold exposure to facilitate the cold-induced adipose tissue beiging process[24]. Here, using a transgenic animal model overexpressing Cx43 in adipocytes and a clinically tested Cx43 channel activator, danegaptide, we demonstrate that activating adipose tissue Cx43 gap junctions potentiates the effects of several pharmacological agents targeting adipose tissue, suggesting a more broadly applicable mechanism of activating Cx43 gap junctions to prime adipose tissue for pharmacological interventions.

2. Materials and methods

2.1. Study approval

Animal care and experimental protocols were approved by the Institutional Animal Care and Use Committee of the University of Texas Southwestern Medical Center (UTSW). The adipose tissue-specific doxycycline-inducible *Gja1* mouse (Adipoq-rtTA:TRE-*Gja1*) was previously generated and characterized in our laboratory[24]. C57BL/6 WT mice were purchased from Jackson Laboratory (Stock No.: 000664). Danegaptide (AdooQ Bioscience, A15092-50) and mirabegron (Sigma−Aldrich, COM497516424-1G) were first dissolved in DMSO before being diluted in PBS and used at 10 mg/kg body weight *via* oral gavage administration. Human FGF21 protein was produced by expressing human FGF21 cDNA in *Escherichia coli*. Protein was purified from the inclusion body by denaturing and refolding. Refolded FGF21 activity was confirmed by a luciferase activity assay. FGF21 was administered at 1 mg/kg body weight *via* intraperitoneal injection. Liraglutide was provided by Novo Nordisk and was administered at 0.2 mg/kg

body weight *via* intraperitoneal injection. Male mice were randomly allocated to experimental groups, and weight-matching was ensured at the beginning of experimental protocols. Investigators were not blinded to treatment groups during studies.

2.2. qPCR

RNA was isolated from frozen tissues by homogenization in Trizol Reagent (ThermoFisher, 15596018) with the manufacturer-provided protocol[25,26]. 1 μg of RNA was used to transcribe cDNA using a reverse transcription kit (Bio-rad, 1708841BUN). RT-qPCR primers are obtained from Harvard PrimerBank[27] (https://pga.mgh.harvard.edu/primerbank/). The messenger RNA levels were calculated using the comparative threshold cycle (Ct) method, normalized to gene *Rps16* or *Gapdh*.

2.3. Western blotting

Protein extractions were performed as previously described[28,29]. Primary antibodies p-ERK (Thr202/Tyr204, Cell Signaling, #4370S; 1:1000 dilution), ERK1/2 (C-9, Santa Cruz Biotechnology, SC-514302; 1:200 dilution), tyrosine hydroxylase (Abcam, ab75875; 1:1000 dilution), adiponectin (rabbit polyclonal, home-made), Connexin43 (Santa Cruz Biotechnology, SC-6560-R) and α-tubulin (DM1A, Cell Signaling, #3873S) were used. Protein abundance was detected using one of the following secondary antibodies: goat anti-mouse IRDye 680RD (LI-COR Biosciences, 926-68070), goat anti-rabbit IRDye 800CW (LI-COR Biosciences, 925-32211) at 1:10,000 dilutions. Antibody decorated membranes were then visualized on a LI-COR Odyssey infrared scanner (LI-COR Biosciences). The scanned data were analyzed using Odyssey Version 3.0 software (LI-COR Biosciences).

2.4. Histology

White adipose tissue, brown adipose tissue, and livers were excised and fixed overnight in 10% PBS-buffered formalin and were thereafter stored in 50% ethanol. Tissues were sectioned (5 μm), rehydrated, and stained in the Pathology Core at UT Southwestern.

2.5. Serum chemistry and ELISA

Serum parameters (aspartate transaminase, alanine transaminase, cholesterol, triglyceride, very low-density lipoprotein, low-density protein, and direct high-density lipoprotein) were measured and calculated with a VITROS analyzer (Ortho Clinical Diagnostics) at the Metabolic Phenotyping Core at UT Southwestern. Mouse serum adiponectin levels were measured using ELISA kits from Millipore (Cat# EZMADP-60K), mouse serum leptin levels were measured using ELISA kits from Sigma−Aldrich (Cat. # GF050).

2.6. Body composition and metabolic cage studies

Body fat mass and lean mass were measured in conscious mice using the Bruker Minispec mq10 NMR (UTSW Metabolic Phenotyping Core). Metabolic cage studies were conducted using a PhenoMaster System (TSE systems) at the UT Southwestern Metabolic Phenotyping Core. Mice were acclimated in temporary holding cages for five days before recording. Food intake, movement, and CO_2 and O_2 levels were measured at various intervals (determined by collectively how many cages were running concurrently) and normalized to body weight for the indicated period shown on figures.

2.7. Mitochondrial respiration

Mice were sacrificed following treatment. Inguinal white adipose tissue was immediately dissected out. Approximately 10 mg of tissue were carved out and weighed, then cut into 3−4 pieces before being placed in an XF24 islet-capture Microplate (Agilent, 103518-100). An insert was placed using the manufacturer-provided tool (Agilent, 101135-100) to prevent floating of the adipose tissue. Mitochondrial oxygen consumption rates (OCRs) from dissected adipose depots were determined using an XF24 Extracellular Flux Analyzer (Seahorse Bioscience, MA, USA) as previously described[30]. The result is normalized to the weight of adipose tissue in each well.

2.8. Lucifer yellow dye coupling

The experimental procedure was described in previous publications[24,31]. Briefly, freshly collected mouse inguinal adipose tissue depots were dissected in patch buffer (110 mmol/L NaCl, 4.7 mmol/L KCl, 14.4 mmol/L $NaHCO_3$, 1.2 mmol/L $MgSO_4$, 1.2 mmol/L NaH_2PO_4, 2.5 mmol/L $CaCl_2$ and 11.5 mmol/L glucose, at pH 7.3 and bubbled with 95% O_2/5% CO_2). Individual adipocytes were visualized under a set up for patch clamp electrophysiology that included an upright microscope (Nikon Eclipse FN1) equipped with a fixed stage and a QuantEM:512SC electron-multiplying charge-coupled device camera. Individual adipocytes were injected with the fluorescent dye Lucifer Yellow (Sigma, L0259-25 MG) 2.5% in 0.5 mol/L LiCl from micropipettes. The dye-injected cells and their neighbor cells were imaged with the digital camera 10 min after the dye injection. Multiple injections from tissues collected from at least five different mice were used for quantification.

2.9. Statistics

All values are expressed as mean ± standard error of mean (SEM). Unpaired Student's *t*-test was used for comparisons of mean values of two groups. F test was used to compare variances. One-way analysis of variance (ANOVA) was used for comparisons of more than two groups. Two-way ANOVA was used to determine the differences between groups that have been split on two independent variables. $P \leq 0.05$ is regarded statistically significant.

3. Results

3.1. Adipose tissue Cx43 overexpression enhances β_3-adrenergic receptor agonist-stimulated mitochondrial respiration and fatty acid utilization

An adipose tissue-specific, doxycycline-inducible Cx43 over-expressing mouse (Cx43 TG) was previously generated by crossing adiponectin promoter driven rtTA mouse to the tetO response element driven *Gja1* mouse[24]. Overexpression of Cx43 in adipocytes of 12-week-old male mice was achieved by supplementing 10 mg/kg of doxycycline in the chow diet (Supporting Information Fig. S1A). Increased Cx43 expression significantly enhanced lucifer yellow diffusion from one adipocyte to the adjacent adipocytes in the inguinal white adipose depot, indicating

increased adipocyte gap junctional activity in those mice (Fig. 1A). To test whether enhanced cellular connectivity can potentiate Mirabegron's effect on mitochondrial respiration, a single oral dose of Mirabegron (10 mg/kg body weight, oral gavage) was given 16 h after transgene induction, 90 min before tissue harvest (Fig. 1B). Fresh inguinal white adipose tissue (iWAT) was immediately prepared for mitochondrial respiration experiments on a Seahorse Instrument (Fig. 1B).

Upon vehicle treatment, fat pads from Cx43 TG mice displayed a comparable oxygen consumption rate to fat pads from littermate control mice. Mirabegron increased oxygen consumption by 36.5% in control fat pads. In contrast, the same dose of mirabegron increased oxygen consumption by 97.4% in Cx43 TG adipose depots, suggesting adipocyte Cx43 expression significantly enhances mirabegron's effect on adipose tissue mitochondrial respiration (Fig. 1C).

A separate cohort of 12-week-old mice were placed in metabolic cages to measure O_2 consumption and CO_2 production to calculate the respiratory exchange ratio (RER) during acute mirabegron treatment. The transgene was induced one day before the metabolic cage experiment, and the mice were maintained on the 10 mg/kg doxycycline high-fat diet (HFD) throughout the study. A single dose of mirabegron treatment increased heat production, suppressed RER, indicating an acute switch from carbohydrate oxidation to fatty acid oxidation in these mice (Fig. 1D, Fig. S1B and S1C). 160 min post-treatment, the RER of the control mice started to recover. In contrast, Cx43 TG mice displayed a prolonged suppression of RER after mirabegron treatment (Fig. 1D). Treatment of Cx43 TG mice with mirabegron also led to a reduction in food intake, which could contribute to the prolonged suppression of RER (Fig. 1E). There was no difference in water consumption (Fig. S1D). Body composition measurement before and after metabolic cage showed a significant smaller gain of fat composition in Cx43 TG mice (Fig. S1E). These data suggest that coupling adipocytes by Cx43 gap junctions augments and prolongs the metabolic effect of β_3-AR agonist mirabegron.

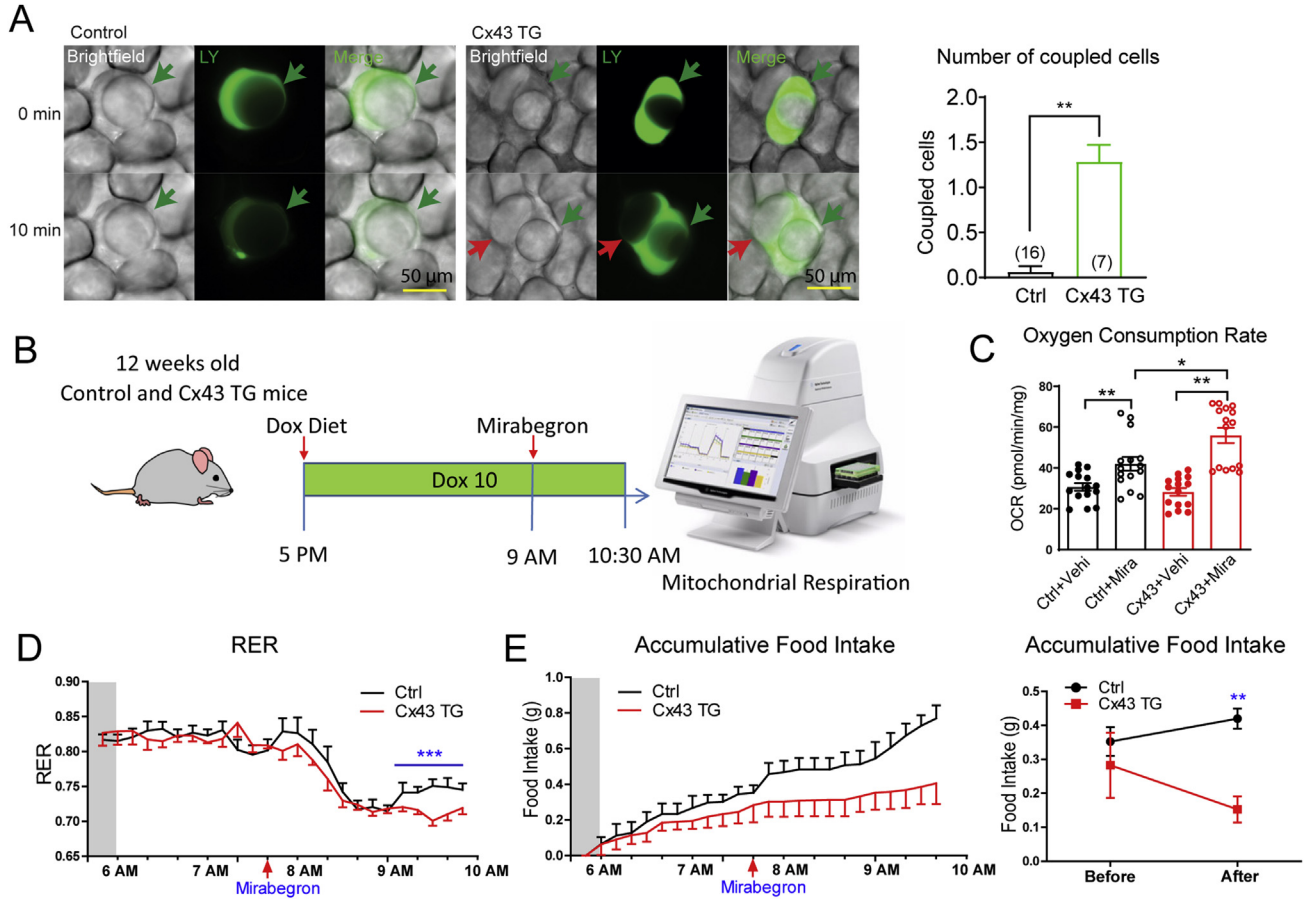

Figure 1 Adipose tissue Cx43 overexpression enhances mirabegron-stimulated mitochondrial respiration and fatty acid utilization. (A) Lucifer yellow (LY) coupling experiments of fresh inguinal white adipose tissue (iWAT) dissected from 12-week-old control (Ctrl) or Cx43 TG mice treated with a chow diet containing 10 mg/kg doxycycline for one week. Quantification of the number of cells coupled to the injected cell is shown on the right (from more than five mice per genotype). (B) Schematic of the experimental design. 12-week-old control (Ctrl) or Cx43 TG mice treated with chow diet containing 10 mg/kg doxycycline at the indicated time. A single dose of mirabegron was administered 90 min before the harvest of the iWAT. (C) Oxygen consumption rates of freshly dissected iWAT measured on a Seahorse instrument (n = 15 pieces fat tissue from five mice). (D) The respiratory exchange ratio (RER) of control (Ctrl) and Cx43 TG mice before and after a single dose oral mirabegron treatment (n = 4−5 mice). Mice were fed a high-fat diet supplemented with 10 mg/kg doxycycline (Dox10 HFD) 24 h before the metabolic cage experiment, and were kept on Dox10 HFD during the metabolic cage recording. The shaded area indicates the dark period during the day. (E) Left: Food intake during the metabolic cage experiment described in Panel D. Right: Accumulative food intake before and after the mirabegron treatment. (n = 4−5 mice). All data are mean ± SEM; *P < 0.05, **P < 0.01, ***P < 0.001.

3.2. *Adipose tissue Cx43 overexpression enhances FGF21's weight loss effect*

Developing β_3-AR agonists as a T2D mediation has been challenging due to safety concerns[15–19]. In contrast, the peptide hormone FGF21 holds great promise, because of its superior safety profile[32]. FGF21 engages the brain and adipose tissue to improve systemic metabolism, and adipose tissue is crucial for FGF21 to exert its metabolic function[33,34]. Intriguingly, overexpressing Cx43 led to enhanced ERK phosphorylation and tyrosine hydroxylase protein content, two main events triggered by FGF21 in adipose tissue (Supporting Information Fig. S2A). To further understand whether this adds to FGF21's metabolic features, we treated a cohort of obese Cx43 TG mice that were exposed to a 12-week HFD regimen. Transgene induction started concurrently with FGF21 treatment. To our surprise, Cx43 overexpression (by supplementing 200 mg/kg doxycycline in HFD) caused 9% weight loss, in contrast to 7.5% weight gain for control mice. FGF21 treatment led to 15.5% weight loss in control mice, and 26.5% in Cx43 TG mice, more pronounced than the added effects of FGF21 treatment and Cx43 overexpression alone (Fig. 2A). The weight loss of Cx43 TG mice with or without FGF21 treatment was at least partially driven by a transient suppression of appetite, which was more evident in Cx43 TG mice treated with FGF21 (Fig. 2A).

In the second cohort of Cx43 TG mice, we lowered the doxycycline in the HFD to 10 mg/kg, and could not see any effects of the genotypes on body weight for 14 days. Subsequently, we switched all mice to HFD containing 50 mg/kg of doxycycline. The body weights of Cx43 TG mice receiving FGF21 treatment showed a divergence compared to FGF21-treated control mice (Fig. 2B). Interestingly, the enhanced weight loss was not attributed to reduced food intake. Cx43 TG mice showed a persistent reduction in food intake, while the Cx43 TG mice treated with FGF21 experienced a transient decrease in food intake but quickly recovered. They showed no difference in food intake after seven days compared to PBS-treated control mice or FGF21-treated control mice (Fig. 2B). Of note, Cx43 expression in iWAT after switching mice to 50 mg/kg doxycycline HFD was 4.3-fold higher in Cx43 TG mice (Fig. S2B), lower than the >10 fold induction by 10 mg/kg doxycycline diet in lean chow-fed mice[24], possibly reflecting a reduction of adiponectin promoter activity and thus also rtTA expression in obese mice. Cx43 TG mice also had lower serum adiponectin levels, and lower leptin levels (Fig. S2C and S2D).

3.3. *Danegaptide enhances mirabegron's metabolic effects, further improving insulin sensitivity and serum lipid profiles*

The genetic manipulation of Cx43 gap junction is difficult, if not impossible in human adipose tissue. However, agonists have been developed to clinically modulate Cx43 gap junctional activity[35]. Danegaptide is a safe compound in research animals and has been tested in Phase I and Phase II clinical trials (Trial numbers: NCT00783341, NCT00510029, and NCT01977755). Pretreatment with danegaptide (10 mg/kg body weight, oral gavage) for 1 h significantly enhanced white adipocyte coupling, as evident by increased lucifer yellow spread (Fig. 3A).

We set out to test whether danegaptide and the previously used β_3-AR agonist mirabegron exert synergistic effects, further improving metabolic parameters. In metabolic cages, pretreatment of 12-week-old C57BL/6J wild-type mice with danegaptide (10 mg/kg body

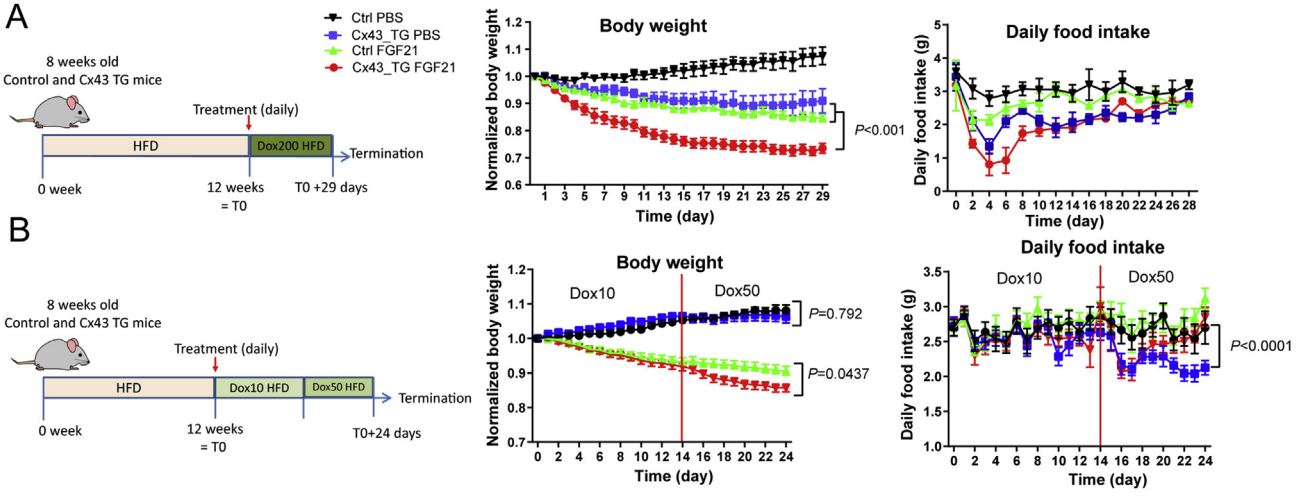

Figure 2 Adipose tissue Cx43 overexpression enhances FGF21's weight loss effects. (A) Weight-loss and food intake of control and Cx43 TG mice treated with PBS or FGF21 (1 mg/kg body weight) on HFD containing 200 mg/kg doxycycline (n = 3–4 mice). 8-week old control or Cx43 TG mice were treated with HFD for 12 weeks to induce obesity, and then both groups were switched to HFD containing 200 mg/kg doxycycline (Dox200 HFD) to induce transgene overexpression and treated with PBS or FGF21 through intraperitoneal injection, daily, for the indicated time. For body weight graph, P value was calculated from two-way ANOVA analysis, indicating the significance of the comparison between indicated groups. (B) Weight-loss and food intake of control and Cx43 TG mice treated with PBS or FGF21 (1 mg/kg body weight) on HFD containing 10 mg/kg doxycycline for 14 days followed by 50 mg/kg doxycycline for additional 10 days (n = 7–9 mice). 8-week old control or Cx43 TG mice were treated with HFD for 12 weeks to induce obesity, and then both groups were switched to HFD containing 10 mg/kg doxycycline (Dox10 HFD) for 14 days, followed by 50 mg/kg doxycycline HFD (Dox50 HFD) treatment. Daily PBS or FGF21 treatment was started at the initiation of Dox10 HFD treatment, through intraperitoneal injection, for the whole duration. For body weight and daily food intake graphs, P values were calculated from two-way ANOVA analysis using data generated on Dox50 HFD treatment, indicating the significance of the comparison between indicated groups. All data are mean ± SEM.

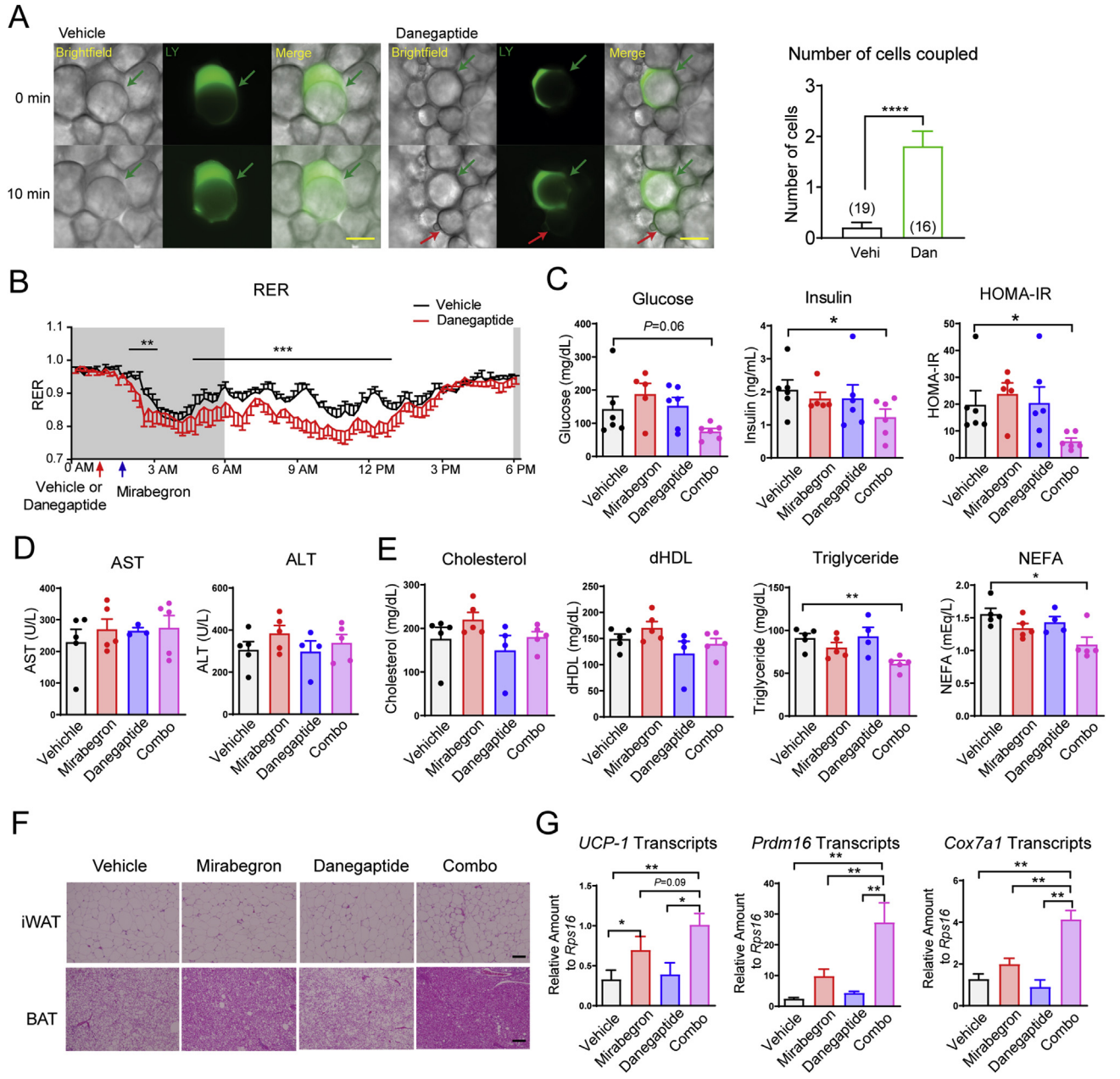

Figure 3 Danegaptide enhances mirabegron's efficacy in improving insulin sensitivity and serum lipid profile. (A) Lucifer yellow coupling experiments of iWAT isolated from 12-week-old normal chow-fed C57BL/6J wild-type mice 1 h after vehicle (Vehi) or danegaptide (Dan, 10 mg/kg body weight) treatment (oral gavage). The number of cells coupled to the injected cell is shown on the right (from at least five mice per treatment). Scale bar = 50 μm. (B) RER of 12-week-old normal chow-fed C57BL/6J wild-type mice treated with danegaptide followed by mirabegron (n = six mice). The shaded area indicates the dark cycle. (C) Insulin sensitivity calculated as HOMA-IR after 9-day daily danegaptide and mirabegron treatment of diet-induced-obese (DIO) C57BL/6J wild-type mice (12 weeks of HFD feeding starting at the age of 8 weeks, n = 5−6 mice). (D) AST and ALT activities after 9-day daily danegaptide and mirabegron treatment of DIO C57BL/6J wild-type mice (12 weeks of HFD feeding starting at the age of 8 weeks, n = 5−6 mice). (E) Serum lipid profiles after 1-week daily danegaptide and mirabegron treatment of DIO C57BL/6J wild-type mice (12 weeks of HFD feeding starting at the age of 8 weeks) (n = 4−5 mice). dHDL: direct high-density lipoprotein; NEFA: nonesterified fatty acids. (F). Representative histology of brown adipose (BAT) and iWAT histology from at least three mice after 1-week daily danegaptide and mirabegron treatment of DIO C57BL/6J wild-type mice (12 weeks of HFD feeding starting at the age of 8 weeks). Scale bar = 100 μm. (G). Adipose tissue beigeing gene expression in the iWAT from 9-day daily danegaptide and mirabegron treatment of DIO C57BL/6J wild-type mice (12 weeks of HFD feeding starting at the age of 8 weeks, n = 10−12 mice). All data are mean ± SEM; $^*P < 0.05$, $^{**}P < 0.01$, $^{***}P < 0.001$.

weight, oral gavage) 1 h before treatment with mirabegron (10 mg/kg body weight, oral gavage) yielded a faster and more prolonged suppression of RER (Fig. 3B and Supporting Information Fig. S3A), similar to what we observed in mirabegron-treated Cx43 TG mice. The effect extended over more than 12 h, spanning the entire light cycle (Fig. 3B). Of note, food consumption, food-seeking activity (Fig. S3B), and overall physical activity (Fig. S3C) were not different between vehicle and danegaptide pre-treatment groups.

In a separate metabolic phenotyping cohort, diet-induced-obese C57BL/6J wild-type mice treated with the danegaptide and mirabegron combination therapy daily for 9 days showed a trend towards serum glucose reduction. Each individual compound did not affect whole-body insulin sensitivity as judged by HOMA-IR, but the combination showed a 68.9% reduction in HOMA-IR in comparison to the control group (Fig. 3C). Serum aspartate aminotransferase (AST) and alanine aminotransferase (ALT) activities were not changed, reflecting hepatic safety of each of the compounds as well as for the combination treatment (Fig. 3D). Total cholesterol and high-density lipoprotein were not altered in any of the treatment groups. Triglycerides and NEFAs showed a statistically significant reduction in the combination group, but not in the individual compound treatment groups (Fig. 3E).

iWAT displayed patches of beige adipocytes only in the combination group. Most strikingly, control mice showed significant brown adipose tissue (BAT) "whitening", which was partially reversed by mirabegron treatment, but displayed an almost full reversal from the unilocular lipid droplet phenotype to the typical multilocular phenotype in the combination treatment group (Fig. 3F). Expression of the adipose tissue beiging marker *Ucp1*, *Prdm16* and *Cox7a1* supported an augmented iWAT beiging in the combination treatment group (Fig. 3G). All these observations suggest a robust metabolic benefit when combining the two compounds.

3.4. *Danegaptide enhances FGF21's metabolic function*

Last, we aimed to address whether combining danegaptide with FGF21 enhances the latter's efficacy. A cohort of diet-induced obese C57BL/6J wild-type mice were treated with FGF21 in combination with danegaptide (Fig. 4A). In the same experiment, we included a liraglutide treatment as a control group that served two purposes: 1) its mechanism of action is at present thought to be independent of a direct effect on adipose tissue, so no synergistic effects would be expected when combined with danegaptide; 2) as an FDA-approved therapy for T2D and a widely-used agent in the class of GLP1 agonists, liraglutide serves as a comparator to gauge the degree of metabolic improvements we can achieve when combing FGF21 with danegaptide.

FGF21 or liraglutide significantly reduced body weight during a treatment period of 16 days. Adding danegaptide to liraglutide prompted no further reductions of body weights. In contrast, combing danegaptide with FGF21 further reduced the body weights and showed no sign of a plateauing effect at the end of the 16-day treatment (Fig. 4B). The weight-loss effect of FGF21 and FGF21 + danegaptide groups were independent of a reduction in food intake, in contrast to liraglutide treatment (Fig. 4B). Adding danegaptide to FGF21 did not further reduce serum AST and ALT enzymatic activity (Supporting Information Fig. S4A). Fasting glucose levels in FGF21 group and FGF21 + danegaptide group were higher when compared to liraglutide treatment, but were still near normal. Despite slightly higher glucose levels, the insulin sensitivity (HOMA-IR) of the FGF21 group and FGF21 + danegaptide group were comparable to the liraglutide group, primarily due to lower serum insulin levels (Fig. 4C). Both FGF21 treatment groups, but particularly the FGF21 + danegaptide group, showed a smaller variance in their HOMA-IR value than the liraglutide group (F-test, $P = 0.02$ for Lir *vs.* FGF21, $P = 0.001$ for Lir *vs.* FGF21 + Dan). In other words, there was a lot less scatter in those groups, with a dramatic reduction in the number of outliers.

Additionally, there was a significant improvement in all four lipid species measured in the serum after adding danegaptide to FGF21 treatment, in comparison to no further reduction when combing denagaptide with liraglutide (Fig. 4D). Serum adiponectin levels were not changed by any treatment (Fig. S4B). Hepatic lipid accumulation was also significantly alleviated in the FGF21 + danegaptide group (Fig. 4E and Fig. S4C). In comparison to control or FGF21 treatment alone, white adipocytes were smaller and brown adipocytes showed a significant reversal of whitening in the FGF21 + danegaptide combination group (Fig. S4D and S4E), which coincided with a significant increase in *Ucp1* expression in BAT (Fig. S4F). Of note, iWAT Cx43 expression was not different (Fig. S4F).

When the cotreatment was extended to 4 weeks in a separate cohort, adding danegaptide to FGF21 led to an additional 6.2% weight loss beyond FGF21's 9.9% weight loss, even in the presence of a compensatory increase in food intake (Fig. S3G). Glucose tolerance did not show any additional differences between the FGF21 and FGF21 + danegaptide groups. However, adding danegaptide significantly lowered fasting insulin and glucose-stimulated insulin levels by 27% (Fig. S4H), suggesting enhanced insulin sensitivity in mice exposed to the combination therapy.

4. Discussion

After a chronic metabolic challenge, adipocyte expansion outpaces vascularization, making them less accessible to endogenous metabolic regulators and pharmacological therapeutic agents[36]. The extraordinarily big size of adipocytes is even likely to trigger the "compartmentalization" of cellular signaling within a cell. Therefore, enhancing the connectivity between adipocytes *via* gap junctions has the potential to augment metabolic and signal exchanges between adipocytes and to amplify neuronal and hormonal input.

Using a rodent model that inducibly overexpresses Cx43 in the adipose tissue upon dietary doxycycline supplementation and a Cx43 gap junction activator danegaptide, we demonstrate that Cx43 gap junctions can enhance β_3-AR agonist's effect on adipose tissue respiration (measured as oxygen consumption) and *in vivo* substrate utilization (measured as RER). Acute mirabegron treatment also leads to rapid suppression of food intake, which is likely mediated by the release of NEFA through adipocyte lipolysis. Danegaptide treatment enhances mirabegon's suppression on food intake, likely through a magnified lipolysis process, which agrees with a lower RER observed in the metabolic cage study. Cx43 overexpression by itself also had a transient suppression effect on food intake, which remains to be elucidated.

Mechanistically, enhanced recruitment of beige adipocytes upon increasing Cx43 gap junction activity is a likely contributor to the enhanced metabolic effects of β_3-AR agonists and FGF21[15]. Beige adipocytes are rich in mitochondria and UCP1 protein[6,7] and have the ability to uncouple mitochondrial respiration from ATP synthesis to burn fatty acids. Other mechanisms, such as the restoration of BAT function, should also play an important role, especially in very obese mice that are resistant to beiging.

Similarly, enhancing adipose tissue gap junction also potentiates FGF21's metabolic effect. Treating diet-induced obese (DIO) mice with danegaptide and FGF21 led to significantly higher weight loss. This synergistic effect was not observed when combing danegaptide with the GLP1 agonist liraglutide. More strikingly, combing danegaptide with FGF21 achieved a better weight loss compared to liraglutide treatment, which is currently one of the gold standards for T2D treatment.

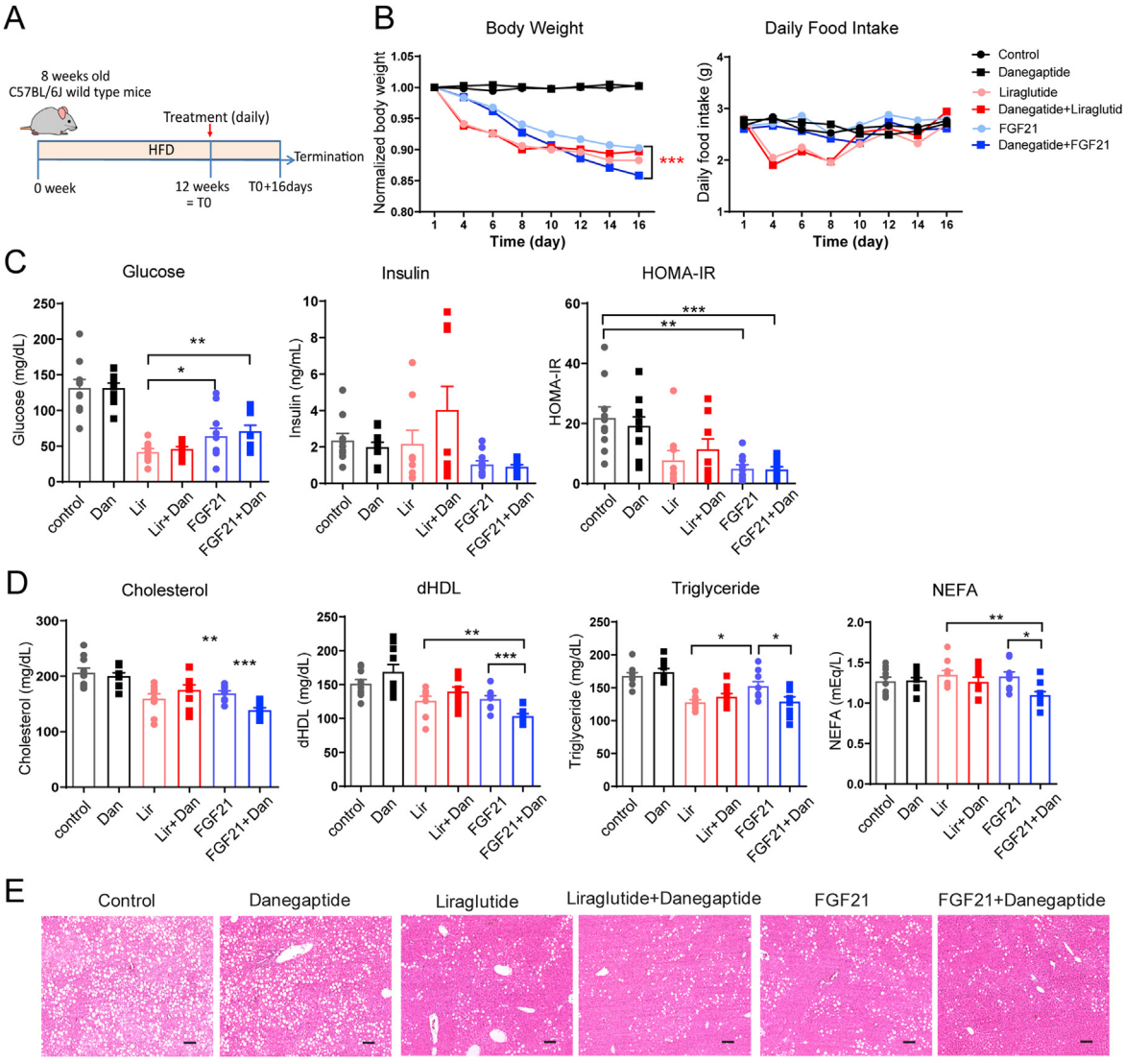

Figure 4 Danegaptide enhances FGF21's metabolic effects. (A) Schematic of the experimental design. 8-week-old C57BL/6J mice were treated with HFD for 12 weeks to induce obesity. Then mice were treated with indicated drugs daily for 16 days; each mouse received vehicle or danegaptide (10 mg/kg body weight) *via* oral gavage, vehicle, or FGF21 (1 mg/kg body weight) or liraglutide (0.2 mg/kg body weight) *via* intraperitoneal injection. (B) Enhanced weight loss after adding danegaptide to FGF21 treatment (left). Food intake during the treatment (right) ($n = 10$ mice). (C) Insulin sensitivity quantified as HOMA-IR after 16-day treatment shown in Panel A ($n = 10$). (D) Fasting serum lipid profile after 16-day treatment shown in Panel A ($n = 10$). dHDL: direct high-density lipoprotein; NEFA: nonesterified fatty acids. (E) Representative histology of the liver from at least three mice after 16-day treatment shown in Panel A. Scale bar = 100 μm. All data are mean ± SEM except for Panel B, in which error bars were removed to enhance the view of the data. $^{*}P < 0.05$, $^{**}P < 0.01$, $^{***}P < 0.001$.

FGF21 was first identified as a novel metabolic regulator during a search for factors enhancing glucose uptake in adipocytes at Eli Lilly in 2005[20]. Because of the high expression of its obligatory receptor *Klb* in adipocytes, most, if not all, FGF21's metabolic benefits were initially assigned to its adipose tissue action. Many studies highlighted a cell-autonomous role of FGF21 in white and brown adipocytes[21,34,37–39]. However, later studies established the role of the central nervous system in FGF21's effect on weight loss[40–42]. These studies revealed that FGF21 activated a sympathetic neuronal signal from the brain to the adipose tissue to promote thermogenesis and weight loss[40]. It is noteworthy that functional adipose tissue is still needed for FGF21's weight-loss effect[34,43].

Based on these studies and our observations of a synergistic effect of danegaptide and FGF21 treatment, we believe FGF21 regulates thermogenesis and weight loss in a coordinated manner, engaging the central nervous system to generate a sympathetic signal to promote thermogenesis and the thermogenic adipose tissue to assimilate glucose to fuel the thermogenic respiration. Simply overexpressing β-Klotho in adipose tissue is sufficient to reduce the weight-gain of mice fed a HFD[44], suggesting endogenous FGF21 action on adipose tissue is limited by the availability of its receptor/co-receptor complexes and its ability to activate them. Coupling adipocytes with Cx43 gap junctions most likely allows more efficient exchange of downstream signaling molecules to improve both FGF21's direct intracellular effects and indirect effects downstream of the sympathetic system. And enhancing adipose tissue substrate combustion *via* adipocyte Cx43 gap junctions can enhance FGF21's overall efficacy.

An increase of BAT tyrosine hydroxylase content in Cx43 TG mice, which is likely a reflection of more sympathetic neuronal fibers in the tissue, is of particular interest. Given FGF21 sends a sympathetic signal from the brain to the adipose tissue, more sympathetic neuronal fiber would allow more inputs of FGF21 signal from the brain to the adipose tissue. However, additional work is needed to understand the molecular mechanism leading to the increase of tyrosine hydroxylase by Cx43 overexpression and whether a similar increase in the BAT tyrosine hydroxylase levels can be observed after danegaptide treatment.

Additionally, a decrease in the scatter, *i.e.*, the variance of HOMA-IR, in FGF21 and FGF21 + danegaptide treatment groups, is especially intriguing. Physiologically, reducing HOMA-IR's variance could be more effective than decreasing the mean HOMA-IR to allow a targeted population of subjects with widely dispersed HOMA-IR values to meet a HOMA-IR threshold. Thus, the reduction in the variance of HOMA-IR in FGF21 and FGF21 + danegaptide treated groups may have big clinical implications, suggesting a larger number of individuals would reach their target HOMA-IR and hence their HbA1C levels with those treatments.

5. Conclusions

In light of these data, we believe connecting adipocytes *via* Cx43 gap junctions allows a more effective exchange of signaling molecules, and it primes adipose tissue to pharmacological interventions. Particularly, the simple combination of danegaptide and mirabegron may enable patients to fully benefit from mirabegron at lower, non-toxic doses and may pave the way for β_3 adrenergic agonists back into the clinic. Future efforts will need to be targeted toward a better understanding of the identity of molecules that pass through the gap junctions and how they effectuate the enhanced metabolic benefits.

Acknowledgments

We thank Steven Connell for technical assistance, the University of Texas Southwestern Medical Center Molecular Pathology Core for assistance in histology, Dr. Syann Lee, Sara Ping, Ellis Cupit, and the Metabolic Phenotyping Core for their help in the metabolic cage studies. This study was supported in part by a research grant from Novo Nordsik (USA, to Philipp E. Scherer) as well as by NIH Grants (USA) R01-DK55758, R01-DK099110, R01-DK127274, R01-DK131537 and P01-AG051459 to Philipp E. Scherer, NIH Grant R00-DK114498 and USDA ARS (cooperative agreement 3092-51000-062) to Yi Zhu, NIH Grant K99-AG068239 to Shangang Zhao, NIH Grant K01-DK125447 to Yu A. An, AHA Career Development Award 855170 (USA) to Qingzhang Zhu, and NIH grants R01 DK119169 and P01 DK119130-5830 to Kevin W. Williams.

Author contributions

Yi Zhu conceived the idea, designed the studies, carried out the research, interpreted the results, and wrote the manuscript. Yu A. An carried out the mitochondrial respiration experiment, Jianhong Cao, Zhenyan He, and Kevin W. Williams carried out the adipocyte lucifer yellow coupling experiment, Na Li, Mingyang Huang, Xi Chen, Jianping Li, Shangang Zhao, Jan-Bernd Funcke, Qingzhang Zhu, and Zhuzhen Zhang assisted in the research. Zhao V. Wang, Lin Xu, Chien Li, and Kevin Grove assisted in study design and provided recourses for the study. Philipp E. Scherer conceived the idea, supervised the study, reviewed and revised the manuscript. All authors approved the final version of the manuscript.

Conflicts of interest

The authors have declared that no conflict of interest exists. K.L.G. and C.L. are employees of Novo Nordisk.

Appendix A. Supporting information

Supporting data to this article can be found online at https://doi.org/10.1016/j.apsb.2022.02.020.

References

1. Khaodhiar L, McCowen KC, Blackburn GL. Obesity and its comorbid conditions. *Clin Cornerstone* 1999;**2**:17–31.
2. White Jr JR. A brief history of the development of diabetes medications. *Diabetes Spectr* 2014;**27**:82–6.
3. Gimeno RE, Moller DE. FGF21-based pharmacotherapy—potential utility for metabolic disorders. *Trends Endocrinol Metabol* 2014;**25**:303–11.
4. Moller DE. Metabolic disease drug discovery—"hitting the target" is easier said than done. *Cell Metabol* 2012;**15**:19–24.
5. Crewe C, An YA, Scherer PE. The ominous triad of adipose tissue dysfunction: inflammation, fibrosis, and impaired angiogenesis. *J Clin Invest* 2017;**127**:74–82.
6. Kusminski CM, Bickel PE, Scherer PE. Targeting adipose tissue in the treatment of obesity-associated diabetes. *Nat Rev Drug Discov* 2016;**15**:639–60.
7. Petrovic N, Walden TB, Shabalina IG, Timmons JA, Cannon B, Nedergaard J. Chronic peroxisome proliferator-activated receptor gamma (PPARgamma) activation of epididymally derived white adipocyte cultures reveals a population of thermogenically competent, UCP1-containing adipocytes molecularly distinct from classic brown adipocytes. *J Biol Chem* 2010;**285**:7153–64.
8. Wu J, Bostrom P, Sparks LM, Ye L, Choi JH, Giang AH, et al. Beige adipocytes are a distinct type of thermogenic fat cell in mouse and human. *Cell* 2012;**150**:366–76.
9. Shinoda K, Luijten IH, Hasegawa Y, Hong H, Sonne SB, Kim M, et al. Genetic and functional characterization of clonally derived adult human brown adipocytes. *Nat Med* 2015;**21**:389–94.
10. Rogers NH, Landa A, Park S, Smith RG. Aging leads to a programmed loss of brown adipocytes in murine subcutaneous white adipose tissue. *Aging Cell* 2012;**11**:1074–83.
11. Hanssen MJ, Hoeks J, Brans B, van der Lans AA, Schaart G, van den Driessche JJ, et al. Short-term cold acclimation improves insulin sensitivity in patients with type 2 diabetes mellitus. *Nat Med* 2015;**21**:863–5.
12. Yoneshiro T, Aita S, Matsushita M, Okamatsu-Ogura Y, Kameya T, Kawai Y, et al. Age-related decrease in cold-activated brown adipose tissue and accumulation of body fat in healthy humans. *Obesity* 2011;**19**:1755–60.
13. Frayn KN, Karpe F. Regulation of human subcutaneous adipose tissue blood flow. *Int J Obes* 2014;**38**:1019–26.
14. Baskin AS, Linderman JD, Brychta RJ, McGehee S, Anflick-Chames E, Cero C, et al. Regulation of human adipose tissue activation, gallbladder size, and bile acid metabolism by a β_3-adrenergic receptor agonist. *Diabetes* 2018;**67**:2113–25.
15. Cypess AM, Weiner LS, Roberts-Toler C, Franquet Elia E, Kessler SH, Kahn PA, et al. Activation of human brown adipose tissue by a β_3-adrenergic receptor agonist. *Cell Metabol* 2015;**21**:33–8.
16. Cawthorne MA, Sennitt MV, Arch JR, Smith SA. BRL 35135, a potent and selective atypical β-adrenoceptor agonist. *Am J Clin Nutr* 1992;**55**. 252S-7S.
17. Weyer C, Tataranni PA, Snitker S, Danforth Jr E, Ravussin E. Increase in insulin action and fat oxidation after treatment with CL 316,243, a highly selective β_3-adrenoceptor agonist in humans. *Diabetes* 1998;**47**:1555–61.

18. Larsen TM, Toubro S, van Baak MA, Gottesdiener KM, Larson P, Saris WH, et al. Effect of a 28-d treatment with L-796568, a novel β_3-adrenergic receptor agonist, on energy expenditure and body composition in obese men. *Am J Clin Nutr* 2002;**76**:780−8.
19. Redman LM, de Jonge L, Fang X, Gamlin B, Recker D, Greenway FL, et al. Lack of an effect of a novel β_3-adrenoceptor agonist, TAK-677, on energy metabolism in obese individuals: a double-blind, placebo-controlled randomized study. *J Clin Endocrinol Metab* 2007;**92**:527−31.
20. Kharitonenkov A, Shiyanova TL, Koester A, Ford AM, Micanovic R, Galbreath EJ, et al. FGF-21 as a novel metabolic regulator. *J Clin Invest* 2005;**115**:1627−35.
21. Fisher FM, Kleiner S, Douris N, Fox EC, Mepani RJ, Verdeguer F, et al. FGF21 regulates PGC-1α and browning of white adipose tissues in adaptive thermogenesis. *Genes Dev* 2012;**26**:271−81.
22. Gaich G, Chien JY, Fu H, Glass LC, Deeg MA, Holland WL, et al. The effects of LY2405319, an FGF21 analog, in obese human subjects with type 2 diabetes. *Cell Metabol* 2013;**18**:333−40.
23. Talukdar S, Zhou Y, Li D, Rossulek M, Dong J, Somayaji V, et al. A long-acting FGF21 molecule, PF-05231023, decreases body weight and improves lipid profile in non-human primates and type 2 diabetic subjects. *Cell Metabol* 2016;**23**:427−40.
24. Zhu Y, Gao Y, Tao C, Shao M, Zhao S, Huang W, et al. Connexin 43 mediates white adipose tissue beiging by facilitating the propagation of sympathetic neuronal signals. *Cell Metabol* 2016;**24**:420−33.
25. Zhu Y, Pereira RO, O'Neill BT, Riehle C, Ilkun O, Wende AR, et al. Cardiac PI3K−Akt impairs insulin-stimulated glucose uptake independent of mTORC1 and GLUT4 translocation. *Mol Endocrinol* 2013;**27**:172−84.
26. Zhu Y, Zhao S, Deng Y, Gordillo R, Ghaben AL, Shao M, et al. Hepatic GALE regulates whole-body glucose homeostasis by modulating *Tff3* expression. *Diabetes* 2017;**66**:2789−99.
27. Wang X, Spandidos A, Wang H, Seed B. PrimerBank: a PCR primer database for quantitative gene expression analysis, 2012 update. *Nucleic Acids Res* 2012;**40**:D1144−9.
28. Zhu Y, Li N, Huang M, Bartels M, Dogne S, Zhao S, et al. Adipose tissue hyaluronan production improves systemic glucose homeostasis and primes adipocytes for CL 316,243-stimulated lipolysis. *Nat Commun* 2021;**12**:4829.
29. Zhu Y, Pires KM, Whitehead KJ, Olsen CD, Wayment B, Zhang YC, et al. Mechanistic target of rapamycin (*Mtor*) is essential for murine embryonic heart development and growth. *PLoS One* 2013;**8**:e54221.
30. Shao M, Ishibashi J, Kusminski CM, Wang QA, Hepler C, Vishvanath L, et al. Zfp423 maintains white adipocyte identity through suppression of the beige cell thermogenic gene program. *Cell Metabol* 2016;**23**:1167−84.
31. Burke S, Nagajyothi F, Thi MM, Hanani M, Scherer PE, Tanowitz HB, et al. Adipocytes in both brown and white adipose tissue of adult mice are functionally connected *via* gap junctions: implications for Chagas disease. *Microb Infect* 2014;**16**:893−901.
32. So WY, Leung PS. Fibroblast growth factor 21 as an emerging therapeutic target for type 2 diabetes mellitus. *Med Res Rev* 2016;**36**:672−704.
33. Lewis JE, Samms RJ, Cooper S, Luckett JC, Perkins AC, Adams AC, et al. Reduced adiposity attenuates FGF21 mediated metabolic improvements in the Siberian hamster. *Sci Rep* 2017;**7**:4238.
34. Veniant MM, Hale C, Helmering J, Chen MM, Stanislaus S, Busby J, et al. FGF21 promotes metabolic homeostasis *via* white adipose and leptin in mice. *PLoS One* 2012;**7**:e40164.
35. Schulz R, Gorge PM, Gorbe A, Ferdinandy P, Lampe PD, Leybaert L. Connexin 43 is an emerging therapeutic target in ischemia/reperfusion injury, cardioprotection and neuroprotection. *Pharmacol Ther* 2015;**153**:90−106.
36. Sun K, Tordjman J, Clement K, Scherer PE. Fibrosis and adipose tissue dysfunction. *Cell Metabol* 2013;**18**:470−7.
37. Chau MD, Gao J, Yang Q, Wu Z, Gromada J. Fibroblast growth factor 21 regulates energy metabolism by activating the AMPK−SIRT1−PGC-1α pathway. *Proc Natl Acad Sci U S A* 2010;**107**:12553−8.
38. Holland WL, Adams AC, Brozinick JT, Bui HH, Miyauchi Y, Kusminski CM, et al. An FGF21−adiponectin−ceramide axis controls energy expenditure and insulin action in mice. *Cell Metabol* 2013;**17**:790−7.
39. Lin Z, Tian H, Lam KS, Lin S, Hoo RC, Konishi M, et al. Adiponectin mediates the metabolic effects of FGF21 on glucose homeostasis and insulin sensitivity in mice. *Cell Metabol* 2013;**17**:779−89.
40. Owen BM, Ding X, Morgan DA, Coate KC, Bookout AL, Rahmouni K, et al. FGF21 acts centrally to induce sympathetic nerve activity, energy expenditure, and weight loss. *Cell Metabol* 2014;**20**:670−7.
41. Lan T, Morgan DA, Rahmouni K, Sonoda J, Fu X, Burgess SC, et al. FGF19, FGF21, and an FGFR1/β-Klotho-activating antibody act on the nervous system to regulate body weight and glycemia. *Cell Metabol* 2017;**26:**709-18.e3.
42. BonDurant LD, Ameka M, Naber MC, Markan KR, Idiga SO, Acevedo MR, et al. FGF21 regulates metabolism through adipose-dependent and -independent mechanisms. *Cell Metabol* 2017;**25**:935−944.e4.
43. Keipert S, Lutter D, Schroeder BO, Brandt D, Stahlman M, Schwarzmayr T, et al. Endogenous FGF21-signaling controls paradoxical obesity resistance of UCP1-deficient mice. *Nat Commun* 2020;**11**:624.
44. Samms RJ, Cheng CC, Kharitonenkov A, Gimeno RE, Adams AC. Overexpression of β-Klotho in adipose tissue sensitizes male mice to endogenous FGF21 and provides protection from diet-induced obesity. *Endocrinology* 2016;**157**:1467−80.